Struct Multidisc Optim (2012) 46:137–153
DOI 10.1007/s00158-012-0761-0

INDUSTRIAL APPLICATION

Sequential robust optimization of a V-bending process using numerical simulations

J. H. Wiebenga · A. H. van den Boogaard · G. Klaseboer

Received: 24 September 2011 / Revised: 11 December 2011 / Accepted: 31 December 2011 / Published online: 31 January 2012

Abstract The coupling of finite element simulations to mathematical optimization techniques has contributed significantly to product improvements and cost reductions in the metal forming industries. The next challenge is to bridge the gap between deterministic optimization techniques and the industrial need for robustness. This paper introduces a generally applicable strategy for modeling and efficiently solving robust optimization problems based on time consuming simulations. Noise variables and their effect on the responses are taken into account explicitly. The robust optimization strategy consists of four main stages: modeling, sensitivity analysis, robust optimization and sequential robust optimization. Use is made of a metamodel-based optimization approach to couple the computationally expensive finite element simulations with the robust optimization procedure. The initial metamodel approximation will only serve to find a first estimate of the robust optimum. Sequential optimization steps are subsequently applied to efficiently increase the accuracy of the response prediction at regions of interest containing the optimal robust design. The applicability of the proposed robust optimization strategy is demonstrated by the sequential robust optimization of an analytical test function and an industrial V-bending process. For the industrial application, several production trial runs have been performed to investigate and validate the robustness of the production process. For both applications, it is shown that the robust optimization strategy accounts for the effect of different sources of uncertainty onto the process responses in a very efficient manner. Moreover, application of the methodology to the industrial V-bending process results in valuable process insights and an improved robust process design.

Keywords Metal forming processes · Finite element method · Optimization · Uncertainty · Robustness · Sequential optimization

J. H. Wiebenga (✉)
Materials innovation institute (M2i), P.O. Box 5008,
2600 GA, Delft, The Netherlands
e-mail: J.Wiebenga@m2i.nl

A. H. van den Boogaard
University of Twente, P.O. Box 217, 7500 AE,
Enschede, The Netherlands
e-mail: A.H.vandenBoogaard@utwente.nl

G. Klaseboer
Philips Consumer Lifestyle, P.O. Box 201, 9200 AE,
Drachten, The Netherlands
e-mail: Gerrit.Klaseboer@Philips.com

1 Introduction

Product improvements and cost reductions are vital in an engineering environment in which the competition increases continuously. The majority of engineering problems encountered in practice, are subject to multiple sources of uncertainty. When dealing with the numerical optimization of metal forming processes using computationally expensive Finite Element (FE) simulations, the challenge is to optimize towards robust metal forming processes. More specifically, the goal is to improve the quality of a product or process by limiting the deteriorating effects of uncertain parameters to an acceptable level.

Neglecting the presence of uncertain parameters will often lead to a deterministic optimum that lies at the boundary of one or more constraints. This situation is schematically shown in Fig. 1a in which the objective function f is

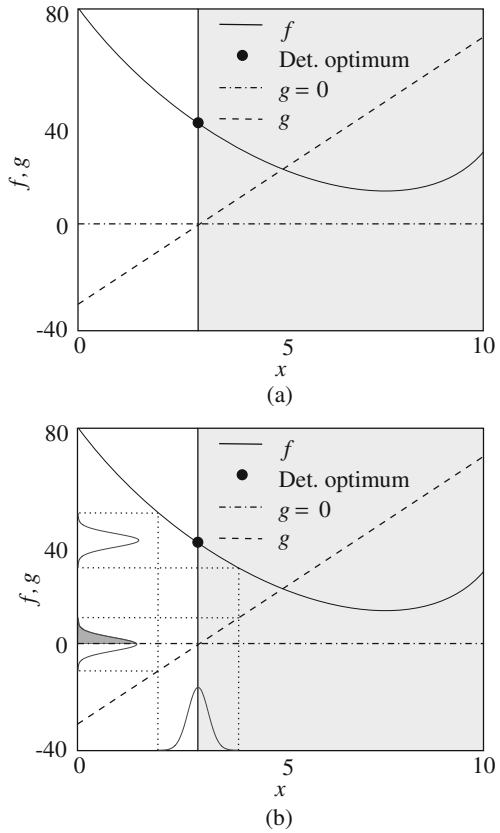

Fig. 1 **a** Deterministic constrained optimization; **b** Robustness of a deterministic constrained optimum where noise is present

minimized subject to the constraint $g \leq 0$. It is assumed here that the design variable can be exactly controlled. Running the FE simulation for selected values of the design variables yields one value for each of both responses f and g.

However, in a real manufacturing environment, the metal forming process is influenced by uncertain parameters or noise variables showing randomness and variability. See e.g. Belur and Grandhi (2004), Hancock et al. (1997) and Padmanabhan et al. (2007). There are different possibilities to classify uncertainties the designer has to deal with, see e.g. Beyer and Sendhoff (2007). This paper specifically considers non-cognitive sources of uncertainty or *aleatory uncertainty* (Haldar and Mahadevan 2000; Möller and Beer 2008). These sources of uncertainty are of physical nature. One can think of the inherent randomness in all physical observations or statistical uncertainty due to lack of precise information about the variation. Extending this to metal forming processes, one can think of changing operating conditions like the scatter of external loads, changing environmental conditions like ambient temperature or variation of material properties.

Noise variables are stochastic variables that can often be described using a probability distribution function. The input variation is translated to the process response (objective and constraints) which will now also display a probability distribution instead of just a deterministic value, see Fig. 1b. Note that half of the response distribution of g violates the constraint $g \leq 0$. Since the constraint represents a sharp border between acceptable products and waste, any presence of variation will now lead to a product rejection rate of approximately 50% in practice.

To avoid such waste, uncertainty has to be taken into account explicitly in any numerical optimization strategy. Figure 2 depicts a diagram which characterizes a manufacturing process such as a metal forming process. It represents the schematic relationship between the input of the process and the response (Yang and El-Haik 2003). The output or response of the process depends on the design variables **x** and noise variables **z**. The output behavior of the system can be controlled by the design variables, e.g. process settings, tooling geometry, etc. The noise variables are the input factors the designer cannot control in an industrial setting, although these cause response variation.

The implementation of uncertainty in a numerical optimization strategy can be achieved in multiple ways. The combination of optimization techniques, numerical simulations and uncertainty is often referred to as *Optimization Under Uncertainty* (OUU), see Schuëller and Jensen (2008). Different approaches are encountered in literature to account for uncertainty.

A first ad hoc approach is to obtain a reliable optimum by optimizing towards a point as far away as possible from the failure constraints. The uncertainties are not accounted for explicitly in this approach. Instead, it is based on the idea of maximizing the minimum distance between the optimal point and failure constraints. This often leads to overdesigned products and does not offer insight into the effects of individual uncertainties and the actual margin of safety.

The prevailing models to account for uncertainty in structural engineering handle noise variables in a probabilistic way. In the Reliability Based Design Optimization (RBDO) approach, an optimal solution of a certain objective function is determined while ensuring a predefined small probability that a product or process fails. A reliability analysis is performed to determine the probability of failure of a design

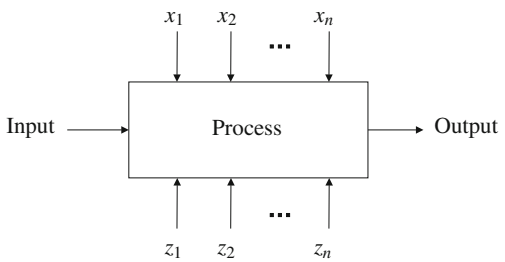

Fig. 2 Process-diagram

with respect to the probabilistic constraints. Applications of the RBDO approach in combination with metal forming processes can be found in Hopperstad et al. (1999), Kleiber et al. (2002, 2004) and Repalle and Grandhi (2005).

In the Taguchi approach, a product or process is called robust if it is minimally sensitive to factors causing variability (Taguchi 1987). The goal of this design philosophy is to minimize the variance of the performance and to drive the mean performance towards a target performance. In contrast to the RBDO approach, reliability is not included explicitly since constraints are not formulated in this approach. An application of the Taguchi approach in the metal forming industry can be found in Kini (2004). Recently, new developments of the hybridization of a genetic algorithm with the Taguchi approach, including design space refinements, are presented in Yildiz et al. (2007) and Yildiz (2009). In these works, the hybrid algorithm is applied for efficiently solving a multi-objective shape design optimization problem of a vehicle component.

In this paper, the robust optimization approach is applied which includes both robustness and reliability of the optimal design. In this approach, an optimal design is characterized by immunity with respect to uncertainty and satisfaction of the constraints. Similar to the RBDO approach, uncertainty or noise variables are accounted for in a probabilistic way. An overview on the most important developments in the field of robust optimization can be found in Beyer and Sendhoff (2007) and Park et al. (2006). Applications of the robust optimization approach in the metal forming industry can be found in Kang (2005) and Li et al. (2005).

In general, the probabilistic OUU approaches result in a deeper understanding of the relationship between design and noise variables with the final part quality. Ultimately, the goal is to improve the quality of a product or process by limiting the deteriorating effects of uncertain parameters to an acceptable level. In many manufacturing settings—also in the metal forming industry—this goal is achieved by application of quality procedures like Statistical Process Control or SPC (Montgomery 2005) and Design for Six Sigma or DfSS (Breyfogle 2003). Similar to the probabilistic OUU approaches, the aspects of robustness and reliability are of fundamental importance in SPC and DfSS. With much of the design process performed in a numerical environment, these aspects have to be included in the numerical design and optimization procedure. However, taking into account the influence of noise variables comes at a computational cost since robust optimization is often much more time-consuming than deterministic optimization. This becomes especially problematic in the case of metal forming processes where computationally expensive FE simulations are used.

In response to this industrial need, a generally applicable strategy for modeling and sequentially solving robust optimization problems is proposed. A number of numerical tools are combined in a framework to efficiently account for the effect of different sources of uncertainty onto the process responses, limiting the required number of FE simulations. First, the concept of robust optimization as applied in this work is introduced in more detail and the relation with SPC and DfSS is outlined in Section 2. Hereafter, the robust optimization strategy is presented in Section 3. To couple the time-consuming FE simulations with an optimization procedure, an approximate optimization approach is applied. The objective and constraints are described in terms of mean values and standard deviations and solved by a global optimization algorithm. The final part of Section 3 is devoted to an in-depth discussion of a sequential robust optimization step used to increase the prediction accuracy of the objective and constraints at regions of interest containing the optimal robust design. By means of two studies, the applicability and efficiency of the strategy is demonstrated. In the first study (Section 4), the robust optimization strategy is applied to an analytical test function. It is demonstrated that adding a sequential optimization step to the robust optimization procedure can further increase the efficiency of the strategy to accurately determine the robust optimum. In the second study (Section 5), these findings are replicated by application of the robust optimization strategy to an industrial V-bending process including experimental validation of the robustness results. Section 6 contains conclusions and provides recommendations for future research.

2 Optimization towards robust and reliable processes

As presented in Figs. 1 and 2, the presence of noise variables as input for the process will cause variation in the responses. Both the noise variables and the responses can be described by a probability density function. Figure 3 shows a normally distributed probability density function of a reference situation with mean μ_f and standard deviation σ_f. Also indicated in Fig. 3 are a Lower and Upper Specification Limit, denoted by LSL and USL respectively.

As mentioned before, process robustness and process reliability are of fundamental importance in SPC. Referring to the Taguchi approach, a product or process is called robust if it is minimally sensitive to factors causing variability. In other words, the robustness can be increased by reducing the variability of the response distribution. The effect of this aspect onto the reference situation is schematically shown in Fig. 3. However, process robustness does formally not include the position of the response distribution with respect to the LSL and USL. In other words, purely minimizing the variability of the response can lead to a very robust process but with a high scrap rate if the

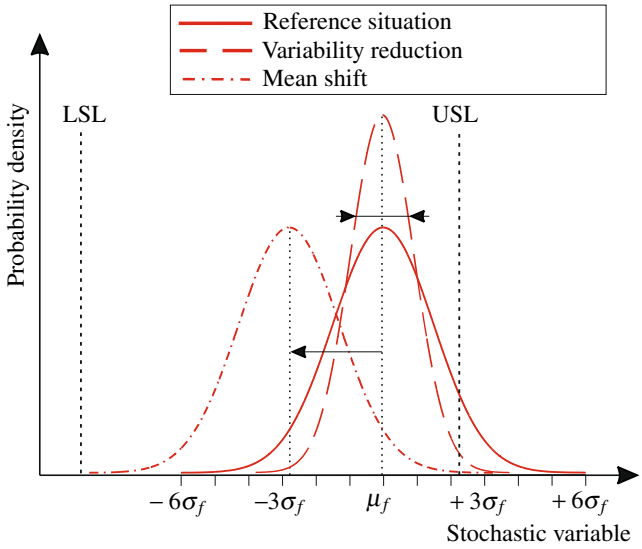

Fig. 3 Variability reduction and mean shift of a reference probability density function

response distribution is located outside the specification limits. Therefore, reliability with respect to the specification limits has to be included in the optimization procedure. Referring to the RBDO approach, reliability is related to the probability that a product or process fails. The probability of failure equals the area in the tail of the distribution that is outside the specification limits. To achieve a certain reliability level, the whole of the probability density function of the response can be shifted until satisfaction of the probabilistic constraints. The violation of the USL can in this case be compensated by adapting the mean of the response distribution, see Fig. 3. Another possibility is to choose the weighted sum of both the mean μ_f and standard deviation σ_f of the response distribution as the optimization objective f. In this case, both the location and the width of the response distribution are adapted simultaneously. To obtain a reliable process, the probability of failure of a design has to be assessed with respect to the constraints $\mathbf{g}$. To reduce the computational burden associated with the evaluation of the probabilistic constraints, a simplified *moment matching formulation* approach is widely used in literature, see Bonte (2007), Du and Chen (2000, 2002), Jin et al. (2003) and Koch et al. (2004). By assuming normally distributed constraint responses, the uncertain constraints can be written as a combination of the mean $\mu_{\mathbf{g}}$ and standard deviation $\sigma_{\mathbf{g}}$. Together, a robust optimization based problem is formulated in the form:

$$\begin{aligned} &\text{find } \mathbf{x} \\ &\min\ f[\mu_f(\mathbf{x}), \sigma_f(\mathbf{x})] \qquad (1) \\ &\text{s.t. } \ \text{LSL} \leq \mu_{\mathbf{g}} \pm \text{k}\sigma_{\mathbf{g}} \leq \text{USL} \end{aligned}$$

Note that using the weighted sum formulation for a constraint can be interpreted as a reliability constraint that ensures a $k\sigma$-reliability with respect to a certain LSL and USL. If g is assumed to be normally distributed, then one can subsequently calculate the scrap rate. For example, $k = 3$ stands for a probability of 0.9973 meaning that 99.73% of the response measurements are within the specification limits which corresponds to a 3σ-reliability. By choosing $k = 6$, one strives for a 6σ-reliability which is the basis of the very successful DfSS quality procedure.

Solving the robust optimization problem defined in (1) requires an efficient approach for determining the response variation and optimal robust design. In this paper, approximate optimization is applied to couple the time-consuming FE simulations with an optimization procedure. Section 3 will presents the key elements of the proposed robust optimization strategy.

3 Robust optimization strategy

In this section, a robust optimization strategy is proposed which is specifically developed for solving optimization problems including time-consuming FE simulations. The strategy is an extension of the deterministic Sequential Approximate Optimization (SAO) algorithm proposed in Bonte et al. (2008). The robust optimization strategy consists of the following main stages: modeling, sensitivity analysis, robust optimization and robust sequential optimization. These main stages can be further subdivided into ten steps, see Fig. 4. This flowchart serves as a guide through the process of mathematically modeling and sequentially solving the robust optimization problem in a structured way.

The robust optimization strategy will be shortly explained by going through the ten steps mentioned in Fig. 4. The key elements and numerical tools incorporated in these steps will be demonstrated in more detail by application to an analytical test function and industrial V-bending process described in Sections 4 and 5 respectively.

3.1 Modeling

The first step (1) in the robust optimization strategy is to model the optimization problem under consideration. Both design and noise variables have to be selected and ranges have to be quantified. For the noise variables, a normal distribution is assumed described by a mean value μ_z and a corresponding variance σ_z^2. The ranges of the design variables $\mathbf{x}$ are bounded by Lower Bounds (**lb**) and Upper Bounds (**ub**). If the design variables can only be controlled to a limited degree in practice, a known or estimated error distribution can be added to account for this uncertainty.

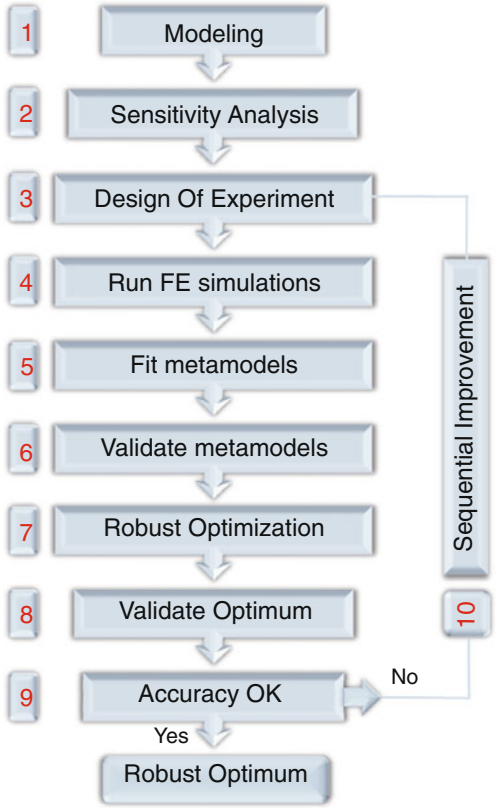

Fig. 4 Flowchart of the robust optimization strategy

The robust optimization formulation used in this work is given by:

$$\begin{aligned} &\text{find } \mathbf{x} \\ &\min \mu_f + k_f \sigma_f \\ &\text{s.t. } \mathbf{LSL} \leq \mu_\mathbf{g} \pm \mathbf{k_g} \sigma_\mathbf{g} \leq \mathbf{USL} \\ &\quad \mathbf{lb} \leq \mathbf{x} \leq \mathbf{ub} \\ &\quad \mathbf{z} \sim \mathcal{N}(\mu_z, \sigma_z^2) \end{aligned} \tag{2}$$

In (2), the objective function is to minimize the weighted sum of both the mean μ_f and standard deviation σ_f of the response. Similarly, the moment matching formulation is used for describing the constraints to ensure a reliable process with respect to the specification limits.

3.2 Sensitivity analysis

Before proceeding with the actual robust optimization procedure, a sensitivity analysis is performed in the second step (2) of the strategy. For industrial metal forming processes, the optimization model obtained in the first step may contain many design and noise variables. As will be reasoned in Section 3.3, a metamodel-based robust optimization algorithm is proposed for solving (2). Metamodels suffer from the so-called curse of dimensionality, i.e. the algorithm becomes exponentially more time-consuming with an increasing dimension of the optimization problem. Screening techniques are therefore applied to reduce the number of variables. This results in a decrease of the size and complexity of the optimization problem, significantly increasing the efficiency of the robust optimization procedure.

The screening techniques used in this work are classical screening techniques as described in e.g. Montgomery (2005, 2009) and Yang and El-Haik (2003). The number of design and noise variables can be reduced based on a fractional factorial Design Of Experiment (DOE) plan (Montgomery 2009). The DOE is applied into a single $(i + j)$-dimensional space for which i and j are the number of design and noise variables respectively. Such a DOE provides an efficient way to obtain *Pareto plots* and *Main Effect plots*, keeping in mind that we are dealing with time-consuming metal forming simulations here. Based on these plots, one can easily determine the most important design and noise variables, i.e. those variables that have the most effect on the responses (objective function and constraints). Taking into account only the design variables that significantly influence the response variation enables a reduction of the number of design and noise variables in the robust optimization problem.

3.3 Robust optimization

The next step is to solve the robust optimization problem defined in (2). Approximate optimization is an often used and well-known approach to couple FE simulations with an optimization procedure. An overview of metamodeling applications in structural optimization was already presented in Barthelemy and Haftka (1993). For the case of robust optimization, approximations have to be generated of the statistical measures of the objective function and constraints in the design space.

Different metamodel-based robust optimization methods can be distinguished, see e.g. Jin et al. (2003) and Myers and Montgomery (2002). In this paper, the *single response surface modeling* approach is applied. At the basis of this approach is a DOE plan in the combined design–noise variable space. When dealing with deterministic computer experiments such as FE simulations, space-filling designs are preferred over other DOE types to minimize the model prediction error (Santner et al. 2003). A typical size of an initial space-filling design for computer experiments exists of 10 times the number of variables (Schonlau 1997). In the third step (3) of the robust optimization strategy, a DOE is created based on a space-filling minimax Latin Hypercube Design (LHD). Figure 5a presents a space-filling LHD of 20 DOE points in the 2D combined design–noise variable space.

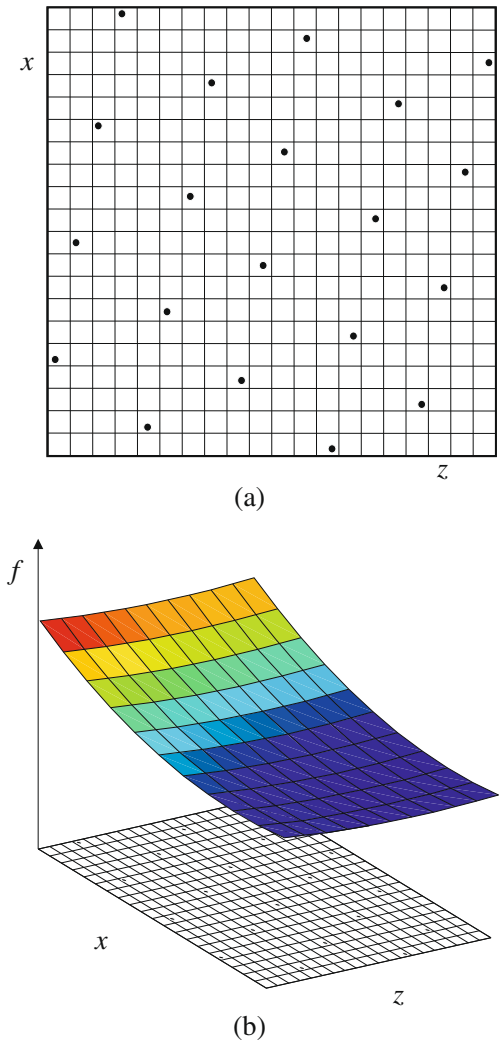

Fig. 5 **a** Space-filling minimax Latin Hypercube Design (*LHD*) in a combined design (x) - noise (z) variable design space; **b** Single response surface model

After running the FE simulations (step 4) corresponding to the settings specified by the DOE, a single metamodel is fitted in the combined space as shown in Fig. 5b. In the robust optimization strategy, the computationally expensive non-linear FE simulations are thus replaced by an approximate model. Since the shape and complexity of the response behavior in the design space is unknown beforehand, both Response Surface Methodology (RSM) and Kriging metamodeling techniques are used for creating a set of approximate models (step 5). The performance of each metamodel is subsequently estimated using ANalysis Of VAriance (ANOVA) techniques (Myers and Montgomery 2002). Validation of the metamodels (step 6) is performed based on leave-one-out cross-validation. Each DOE point is selected once as the validation data, and the remaining DOE points as the training data. The level of fit of each metamodel is calculated and used to select the most accurate metamodel with respect to the FE model response.

From the single metamodel of each response, two approximate models of the response mean $\hat{\mu}_f$ and standard deviation $\hat{\sigma}_f$ are subsequently extracted providing the statistical measures required for the robust optimization procedure. This can be done analytically in case of a RSM metamodel, see Montgomery (2005). When Kriging is employed instead of RSM, an analytical derivation of $\hat{\mu}_f$ and $\hat{\sigma}_f$ is not possible. In this case, a Monte Carlo Analysis (MCA) of 10.000 function evaluations is run multiple times on the metamodel resulting in a model for $\hat{\mu}_f$ and $\hat{\sigma}_f$ as a function of the design variables. Since the MCA is performed on a metamodel, it is very efficient. Both models can now be used for robust optimization (step 7) by applying a global optimization algorithm such as a Genetic Algorithm (GA) to solve (2).

Initially, a small number of DOE points is chosen in the third step of the strategy to limit the required number of expensive function evaluations. The design engineer must be aware of the fact that the solution of the approximated problem is only an estimate of the true robust optimum. To obtain an accurate and reliable solution, the optimal metamodel prediction has to be validated (step 8). In case of a deterministic optimum, this can be done by performing a single FE simulation. In case the robust optimum needs to be validated after optimization, it is necessary to locally run multiple time-consuming FE simulations. Obviously, only a limited number of simulations can be performed resulting in a coarse (and expensive) estimation of the prediction accuracy of the metamodel (step 9). If the accuracy is not sufficient according to the design engineer, a sequential improvement step can be applied to update the metamodel successively (step 10).

3.4 Robust sequential optimization

The goal of sequential optimization is to increase the accuracy of the response prediction at regions of interest containing the optimal design. This is achieved by adding new DOE points to the original set. See e.g. Jakumeit et al. (2005) for an application in metal forming processes. An update algorithm is required to select the location of the next infill point. After evaluating the new infill point by an FE simulation, the metamodels are globally updated and validated taking into account the additional response. A robust optimization procedure is started and the new prediction of the robust optimum is determined. Instead of validating this optimum using FE simulations, a stopping criterion related to the update algorithm is evaluated. The sequential improvement strategy continues to add DOE points until the stopping criterion is fulfilled. As a final check, the design engineer can validate the metamodel prediction accuracy in the vicinity

of the newly predicted robust optimum using FE simulations. In Section 3.4.1, a deterministic update algorithm will be introduced first. An extension of this algorithm to account for the influence of noise variables is subsequently presented in Section 3.4.2.

3.4.1 Expected improvement criterion

In Jones et al. (1998) and Schonlau (1997), a deterministic update algorithm is proposed based on the principle of *Expected Improvement* (EI). The proposed Efficient Global Optimization (EGO) strategy adds additional sample points by maximizing the EI. In general, the Improvement (I) is defined as:

$$\mathrm{I}(\mathbf{x}) = \begin{cases} 0 & \text{if } y(\mathbf{x}) > f_{\min} \\ f_{\min} - y(\mathbf{x}) & \text{otherwise} \end{cases} \tag{3}$$

The improvement is calculated by taking the difference between a function value $y(\mathbf{x})$ with respect to the minimum feasible tested (or calculated) response of the true objective function value $f_{\min}$ if $y(\mathbf{x}) < f_{\min}$. In case a metamodel is used, the function value $y(\mathbf{x})$ can be replaced by a mean value prediction $\hat{y}(x_0)$ at an untried setting x_0. Moreover, in case of deterministic optimization, the function value $\hat{y}(x_0)$ is a direct prediction of the objective function value $\hat{f}(x_0)$.

In addition to the mean value prediction $\hat{y}(x_0)$, the EI algorithm makes use of the *prediction error* $s(x_0)$ provided by the metamodel. In other words, the predictor $\hat{y}(x_0)$ represents a realization of a stochastic process Y in which the randomness is governed by the uncertainty $s(x_0)$ about the true objective function. See e.g. Sacks et al. (1989) and Santner et al. (2003). Note that $s(x_0)$ represents a type of uncertainty that is related to the metamodel prediction which is different from the aleatory type of uncertainty discussed in the introduction of this paper. The so-called *posterior distribution* Y at x_0 can be modeled as a normal distribution with $Y \sim \mathcal{N}(\hat{y}(x_0), s^2(x_0))$.

Replacing $y(\mathbf{x})$ in (3) by the stochastic variable Y will result in an expression of the improvement that is also a stochastic variable. As shown in Jones et al. (1998), the expected value of the improvement can now be expressed in a closed form given by:

$$\mathrm{E}(I) = \begin{cases} (f_{\min} - \hat{y})\,\Phi\left(\dfrac{f_{\min} - \hat{y}}{s}\right) + s\phi\left(\dfrac{f_{\min} - \hat{y}}{s}\right) & \text{if } s > 0 \\ 0 & \text{if } s = 0 \end{cases} \tag{4}$$

with ϕ and Φ the probability density and cumulative distribution function of the standard normal distribution respectively. For notational simplicity, the dependence on $\mathbf{x}$ is omitted here. The first term in (4) contributes to the EI if $\hat{y}$ is smaller than $f_{\min}$. The second term contributes to the EI at locations of high uncertainty about whether $\hat{y}$ will be better than $f_{\min}$. The criterion is thus capable of searching both locally (first term) and globally (second term). Maximizing the EI finally provides the coordinates of the infill point $\mathbf{x}'$.

3.4.2 Extension of the expected improvement criterion

In the case of robust sequential optimization, the goal is to find a suitable location of the infill point which requires the determination of an optimal setting for both the design variables $\mathbf{x}'$ and noise variables $\mathbf{z}'$. Focusing on the EI algorithm, two difficulties arise if noise variables are taken into account. Firstly, the goal is to find an infill point that is most promising with respect to the robustness criterion instead of the metamodel itself. Secondly, the prediction uncertainty or suitable error estimation s associated with respect to the objective function is not accounted for.

Only a few studies have been published that consider sequential update strategies in which noise variables are taken into account, see Huang (2005), Lehman (2002) and Williams et al. (2000). The robust sequential optimization algorithm that is applied in this work is proposed in Jurecka et al. (2007). The search for an infill point in the design–noise space is divided into two steps. First, $\mathbf{x}'$ is determined in the design variable space after which $\mathbf{z}'$ is identified in the noise space. Determining $\mathbf{x}'$ requires the evaluation of the robust objective function f. This is done by application of a MCA onto the metamodel. As a result, the majority of the MCA sampling points that are incorporated in the prediction of the robustness criterion are untested, i.e. not evaluated using a FE simulation. An uncertainty s about the predictor $\hat{y}$ at each untested point $(\mathbf{x}, \mathbf{z})$ remains present. As a result, two stochastic variables are obtained in the same probability space. Each point $(\mathbf{x}, \mathbf{z})$ is now a realization of the stochastic noise variable Z and the posterior error distribution in this point. The stochastic process Y can now be written as $(Y|Z) \sim \mathcal{N}(\hat{y}(Z), s^2(Z))$. To evaluate the prediction uncertainty with respect to the robustness criterion, the conditional variance formula is used:

$$\mathrm{var}(Y) = \mathrm{E}\left(s^2(Z)\right) + \sigma_{\hat{Y}}^2 \tag{5}$$

The presence of prediction uncertainty adds an additional term to the prediction variance of the stochastic process Y which equals the expected value of $s^2(Z)$ over the noise space. This value can be determined by the same sampling methods used to calculate the robustness criterion.

Returning back to the definition of the EI, a revision has to be done. This is because the definition of the current best solution of the robustness criterion can now also be seen as a

stochastic process with $(Y^*|Z) \sim \mathcal{N}(\hat{y}^*(Z), s^{*2}(Z))$. The EI can now be written as:

$$\mathrm{E}(I) = \int_a^b (\hat{y}^* - y)(p_Y(y) - p_{Y^*}(y))dy \tag{6}$$

with $p_Y(y)$ and $p_{Y^*}(y)$ the probability density function of the stochastic process Y and current best solution Y^* respectively. The integration bounds a and b depend on the intersection points of $p_Y(y)$ and $p_{Y^*}(y)$ which can be calculated analytically.

As a first step, the current best solution is calculated by evaluating the robustness criterion for all settings of the design variable $\mathbf{x} = \mathbf{x}_l$ that are part of the set of DOE points. The robustness criterion can now be calculated according to its definition, e.g. $f = \mu_Y + k\sigma_Y$, and its optimal 'tested' value can be determined. Subsequently, the EI can be maximized by evaluating (6) for a set of points $\mathbf{x}$ representing the candidate infill points in the design variable space. In exploring the noise space, the deteriorating effects of the noise variables are of special interest. Maximizing the product of the error prediction and the probability of occurrence results in the optimal noise variable setting:

$$\mathbf{z}' = \arg\max(s^2(\mathbf{x}', \mathbf{z})p_Z(\mathbf{z})) \tag{7}$$

Together, these optimal settings $(\mathbf{x}', \mathbf{z}')$ define the infill point at which a new FE simulation is performed. The resulting FE response is added to the set of responses and the metamodel is updated. The update sequence continues until a threshold value for the EI or a maximum number of runs is reached. In this work, the above described algorithm will be applied adding a single new infill point per iteration. This will result in the most efficient analysis since the metamodel, and with that the EI, is updated each iteration of the algorithm. However, from a practical point of view it may be beneficial to increase the number of infill points per iteration. For example, in case parallel computing facilities are available or if different research groups work separately on the FE-modeling and optimization side of the problem. To do so, one can make use of the multimodal behavior of the EI by adding infill points at multiple maxima. Evaluating the FE-simulations in parallel and updating the metamodel can now be performed at the cost of a single FE-simulation and will reduce the number of required iterations between research groups.

4 Application to an analytical test function

The robust optimization strategy presented in Section 3 allows for modeling and sequentially solving robust optimization problems using time-consuming simulations. The performance of the proposed strategy is demonstrated in this section by the robust optimization of an analytical test function. The Branin function is a classical deterministic optimization test function with 3 global optima. To use the Branin function for robust optimization purposes, one of the two parameters is considered to be a noise variable:

$$y(x, z) = \left(z - \frac{5x^2}{4\pi^2} + \frac{5x}{\pi} - 6\right)^2 + 10\left(1 - \frac{1}{8\pi}\right)\cos(x) + 10 \tag{8}$$

The design space is limited to $-5 \leq x \leq 10$. The noise variable is assumed to follow a normal distribution according to $z \sim \mathcal{N}(\mu_z, \sigma_z^2)$ with $\mu_z = 7.5$ and $\sigma_z = 2.5$. A graphical representation of the Branin function is given in Fig. 6.

As an objective of the optimization study, it is chosen to minimize $f = \mu_y + 3\sigma_y$. The reference solution is obtained beforehand by performing MCA's of 10.000 samples at an equidistant grid of 100 design variable settings using the analytical function. An impression of the reference solution is represented by the solid line in Fig. 7a. Note that the 3 global optima of the deterministic Branin function reduce to a single global robust optimum if one of the two parameters is considered to be a noise variable. The global robust optimum is visualized by the cross mark in Fig. 7a at $x_{\mathrm{ref}} = -1.4$ with an optimal objective function value of $f_{\mathrm{ref}} = 48.6$, see Table 1.

The Branin function is first evaluated based on an initial space-filling LHD of only 10 DOE points. Using ANOVA, an ordinary Kriging model is identified as the most accurate fit for the Branin function. An initial objective function prediction of the Kriging model is obtained in a similar manner as the reference model. See the dotted line in Fig. 7a. The Kriging model is subsequently used for robust optimization by application of a GA optimization algorithm in combination with a MCA. The initial approximation of the optimal objective function value is found to be $\hat{f}_{\mathrm{opt}} = \hat{\mu}_y + 3\hat{\sigma}_y =$

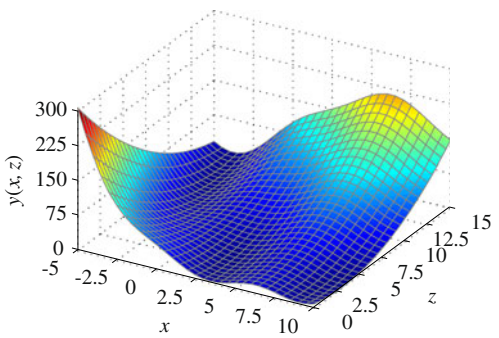

Fig. 6 Graphical representation of the Branin function

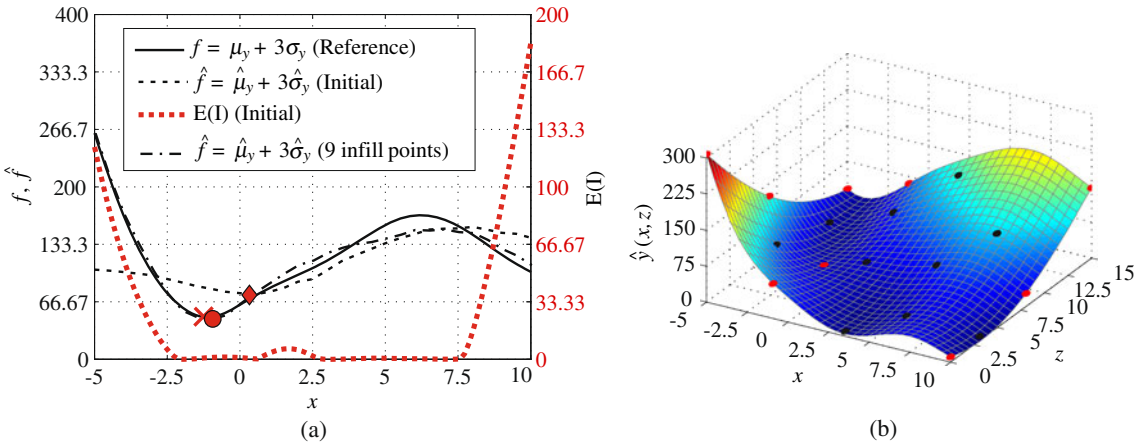

Fig. 7 **a** Reference objective function, Expected Improvement (*EI*) and approximated objective function after 0 (*initial*) and 9 infill points. **b** Kriging model approximation span up by 10 original DOE points (*black markers*) and 9 additional infill points (*red markers*)

74.5 at the design variable setting $x_{\text{opt}} = 0.4$. See the diamond marker in Fig. 7a and Table 1.

A significant deviation of both the optimal objective function value and the optimal design variable setting is observed by comparing the reference values f_{ref} and x_{ref} with the initially obtained values of $\hat{f}_{\text{opt}}$ and x_{opt}. The sequential robust optimization procedure is therefore applied to increase the accuracy of the objective function prediction. The EI, calculated based on the initial Kriging model, is given in Fig. 7a. Maximizing the EI results in the design variable coordinate $x' = 10$ of the first infill point. Evaluation of (7) results in the noise variable setting $z' = 15$. After determining the response at the location $(x', z') = (10, 15)$, the metamodel is updated. As a result, also the prediction error and the EI are revised. This procedure is repeated until the stopping criteria ($\max \text{E}(I) < \Delta_s$) is met, in this case set to $\Delta_s = 0.1$. In total 9 infill points are added after which the EI drops below the threshold. The final result after 9 infill points is depicted in Fig. 7a and b.

The focus of the update algorithm varies between a global search, resulting in infill points at the boundaries of the design variable domain, and a local search in x. The local search converges to the robust optimum, resulting in 3 infill points in the vicinity of $x_{\text{ref}} = -1.4$. Evaluating the robust optimum using the final metamodel (build up out of 10 original DOE points and 9 additional infill points), an optimal value of the robustness criterion of $\hat{f}_{\text{opt}} = 46.9$ is found for $x_{\text{opt}} = -1.3$. See the circular marker in Fig. 7a and Table 1. From this, it can be concluded that the accuracy of the robustness criterion prediction in the vicinity of the robust optimum has been improved significantly by sequentially adding 9 infill points.

As a comparison, the robust optimization procedure is repeated with an initial LHD of 19 points. The optimal objective function prediction, based on the resulting initial Kriging model, is determined at $\hat{f}_{\text{opt}} = 56.6$ for $x_{\text{opt}} = -1.0$. This prediction is less accurate compared to the prediction based on 10 initial DOE points and 9 additional infill points added by the EI update algorithm. Based on the results summarized in Table 1, it is shown that the prediction accuracy increases more rapidly by placing the infill points at qualified locations compared to increasing the initial size of the LHD for the Branin test function. The next step is to verify this finding by application of the sequential robust optimization strategy to an industrial V-bending process.

Table 1 Optimal objective function values and design variable settings for the Branin test function

	f_{ref}	x_{ref}
Reference solution	48.6	−1.4

DOE size	$\hat{f}_{\text{opt}}$	x_{opt}
10 initial LHD points	74.5	0.4
10 initial LHD points + 9 seq. added points	46.9	−1.3
19 initial LHD points	56.6	−1.0

5 Application to an industrial V-bending process

The proposed sequential robust optimization strategy will now be applied to optimize a V-bending process. The industrial application is performed in cooperation with Philips Consumer Lifestyle. An impression of the production process and final product is shown in Fig. 8. A piece of sheet metal is placed in between a punch (upper tool) and

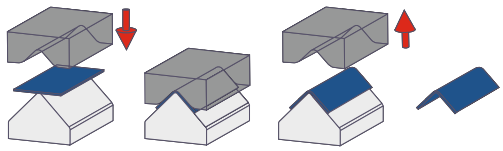

Fig. 8 Impression of the V-bending process and final product

a die (lower tool), after which the punch is lowered by a prescribed displacement. During the bending process, the material experiences local elastic and plastic deformation. After withdrawal of the punch, the product shows elastic springback. The challenge of this study is to optimize the process such that products are produced within specifications in a robust way subject to variation in material behavior. Moreover, the goal is to demonstrate the efficiency and applicability of the strategy and to gain more insight in the effect of noise variables onto the production process.

Figure 9a shows the FE model of the part and tools. A 2D model is created assuming a plane strain condition. The implicit code MSC Marc has been used as FE-code. Due to symmetry of the product, only one half of the geometry has been modeled. The sheet metal is discretized using 500 quadrilateral elements with 5 elements through the thickness. Both the die and punch are modeled to be non-rigid using quadrilateral elements. Considering deformable tools is in this case essential for an accurate simulation. One simulation takes about 7 minutes. The complexity of the FE model, and with that the calculation time, is intentionally limited for the purpose of this research.

The product material is a stainless steel for which the nominal material properties are obtained by uni-axial tensile tests performed at room temperature. The material is modeled as an elastic-plastic material. For the elastic material behavior, a Young's modulus (E) of 210 MPa is used. The material hardening is isotropic and the Von Mises yield criterion is applied. The experimentally obtained true-stress—true-strain curve is implemented in the FE-model as a table to describe the plastic material behavior. The materials yield stress (σ_y) is determined at 350 MPa. Variation in σ_y is modeled by vertically shifting the true-stress—true-strain curve. The tooling material is a tool steel for which only the elastic material behavior is modeled using $E = 210$ MPa.

5.1 Modeling and sensitivity analysis

The initial set of design and noise variables is shown in Fig. 9b. The design variables are the angle of the die and the punch (α), the width of the product (W), the final distance (D) between the flange of the die and punch (if no deformation of the tooling would occur), the dimensions of the punch (L_1) and the die (L_2), the radius of the die (R_1) and punch (R_2). As with the process in practice, the material thickness (M) and yield stress (σ_y) are considered uncertain.

To ensure a correct performance of the final product, constraints on the flange shape are prescribed. The flange shape is defined by a transition angle (θ_T) and a main angle (θ_M) spanned up by the marked line segments; see Fig. 9c. The constraint on the main angle is stricter since this angle is most critical with respect to the performance of the final product. In the current V-bending process, active steering of D is required to obtain products that satisfy the requirements for both angles. The goal of the optimization study is to obtain a robust and reliable process design for the main and transition angle without the need to adjust D. The main angle is taken into account as the objective function

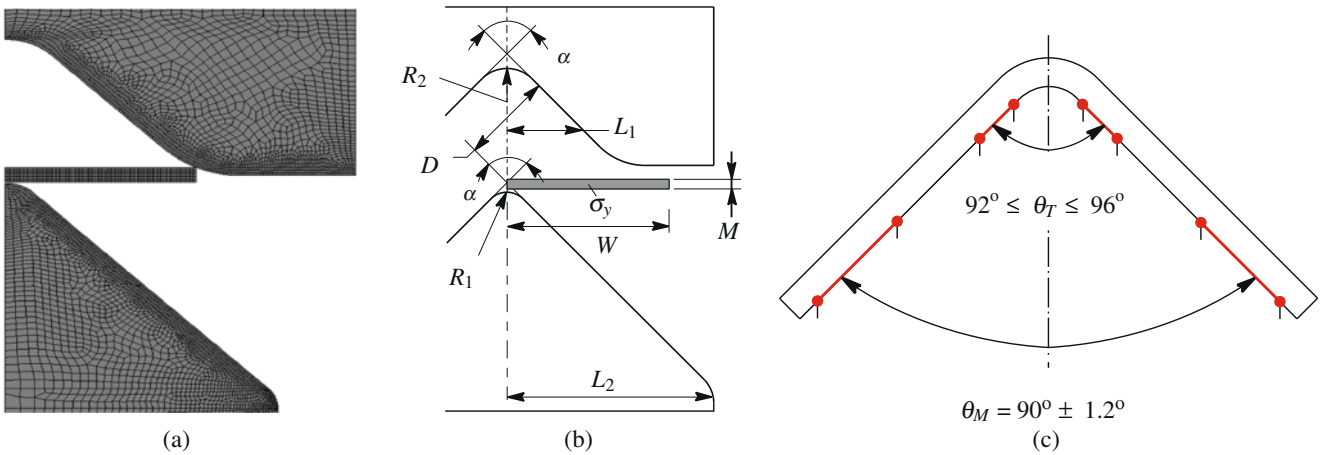

Fig. 9 **a** 2D FE model of the V-bending process, **b** definition of design and noise variables **c** and constraints on the flange shape of the final product

f while satisfying $\pm 3\sigma$-constraints on the transition angle. The quantified robust optimization formulation is given by:

$$
\begin{aligned}
&\text{find } \mathbf{x} \\
&\min\ |(\mu_{\theta_M} - 90)| + 3\sigma_{\theta_M} \\
&\text{s.t. } 92 \leq \mu_{\theta_T} - 3\sigma_{\theta_T} \\
&\quad \mu_{\theta_T} + 3\sigma_{\theta_T} \leq 96 \\
&\quad 92 \leq \alpha \leq 93 \\
&\quad 6 \leq W \leq 7.5 \\
&\quad 0.4 \leq D \leq 0.65 \\
&\quad 4 \leq L_1 \leq 5 \\
&\quad 8.5 \leq L_2 \leq 11 \\
&\quad 1 \leq R_1 \leq 1.3 \\
&\quad 1.8 \leq R_2 \leq 2.1 \\
&\quad M \sim \mathcal{N}(0.51, 0.01^2) \\
&\quad \sigma_y \sim \mathcal{N}(350, 6.66^2)
\end{aligned}
\tag{9}
$$

A sensitivity analysis is first performed to reduce the size and complexity of the optimization problem. The applied screening techniques are discussed in Section 3.2. A resolution IV fractional factorial design of 32 experiments is used for independently estimating the linear main effects of the 9 control and noise variables. The upper and lower bound of the noise variables are set at $\mu + 3\sigma$ and $\mu - 3\sigma$, respectively. The resulting Pareto plots of the objective function and constraint are presented in Figs. 10a and b respectively. Similar to what is experienced in the production process, the sensitivity study shows that the depth setting D has the largest effect on both the objective function and constraint. Moreover, the main and transition angle are highly sensitive to the bending radius R_1, bending angle α and the variation in material thickness M. The change in the dimension of the punch L_1 and variation of the yield stress σ_y only affects the objective function and hardly affects the constraint. Design and noise variables having a higher effect on the objective or constraint than the error effect (dotted line in the Pareto plots) are considered significant and are included in the optimization problem. As a result, the number of variables is reduced to 4 design variables (D, L_1, R_1, α) and 2 noise variables (M, σ_y). The omitted variables (R_2, L_2 and W) are set to their nominal process settings to minimize the required changes in the current production process.

The significance of these variables is verified using experimental data for the V-die bending process available in literature. Leu and Hsieh (2008) recognize the strong influence of increasing the coining force to reduce springback after unloading. This corresponds to decreasing the depth setting in the current work to a value for D which is smaller than the nominal material thickness. The significant effect of D is also experimentally verified in Tekaslan et al. (2008) and Osman et al. (2010). Moreover, experimental results reported in Tekaslan et al. (2006, 2008) and Huang and Leu (1998) for the main angle confirm the importance of the bending radius R_1, material thickness M, and bending angle α. Lastly, the importance of material properties σ_y is experimentally verified in Osman et al. (2010). Varying the dimension of the punch L_1 is not considered in these experimental works although Fig. 10a shows that the effect on the main angle is significant. Further experimental verification of the numerical results will be described in Section 5.4.

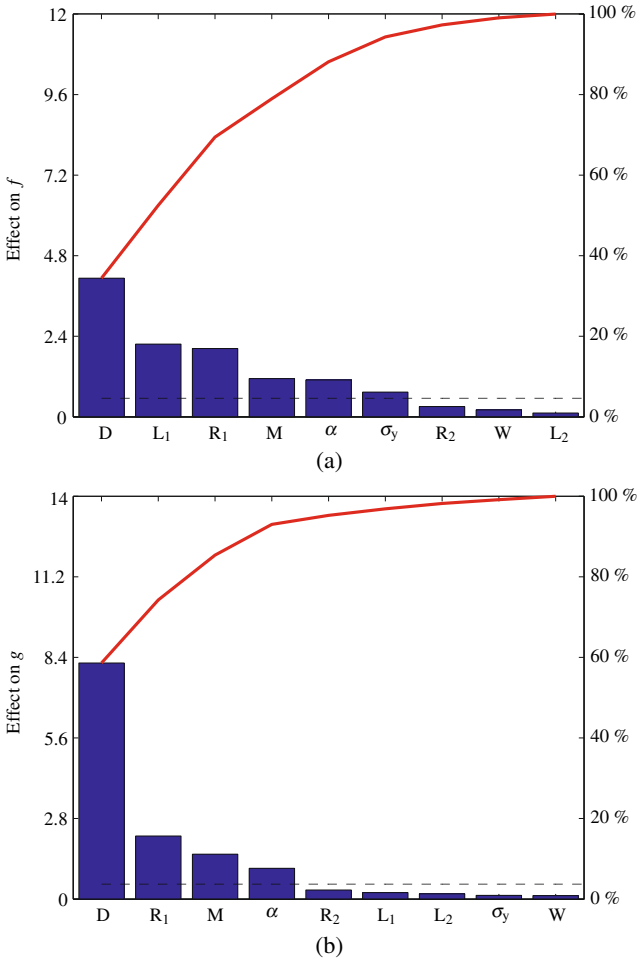

Fig. 10 Pareto plots plots of the **a** objective function f and **b** constraint g

5.2 Metamodel creation

The next step is the creation of metamodels to study higher-order and interaction effects between variables and to perform robust optimization upon. Following the rule of thumb mentioned in Section 3.3, a LHD of $N = 10n$ points is generated, where the reduced number of variables n equals

Table 2 Number of points per dimension used to create a grid of 6000 points in the design space

Dimension	α	R_1	L_1	D	M	σ_y
Number of points per dimension	4	5	4	5	5	3

6 in this case. The resulting 60 points are distributed in the combined 6D design–noise variable space and serve as a basis for the initial metamodel. The FE simulations are performed on four parallel processors reducing the total calculation time to approximately two hours. Using ANOVA, a second-order Kriging model is identified as the most accurate fit for both f and g. In addition to this metamodel, four Kriging models are constructed based on an initial LHD of 30, 100, 200 and 300 points to investigate the influence of the initial DOE size. Moreover, a large reference data set is constructed by performing 6000 FE simulations in the combined 6D design space. These simulations are performed according to a predefined grid. The points per dimension of the grid are distributed in an equidistant manner. The number of points per dimension is presented in Table 2. A reference model is subsequently obtained by spline interpolation of the resulting response set. In the remainder of this paper, these models are referred to as 30LHD, 60LHD, 100LHD, 200LHD, 300LHD and reference model.

The reader should be aware that for this simple case a reference model is created for validation purposes with a lot of computational effort. However, a reference model will not be available in realistic problems. The goal of the (sequential) robust optimization is to calculate the robust optimum with a low number of FE simulations. With the reference model available, the performance of the algorithm can be checked.

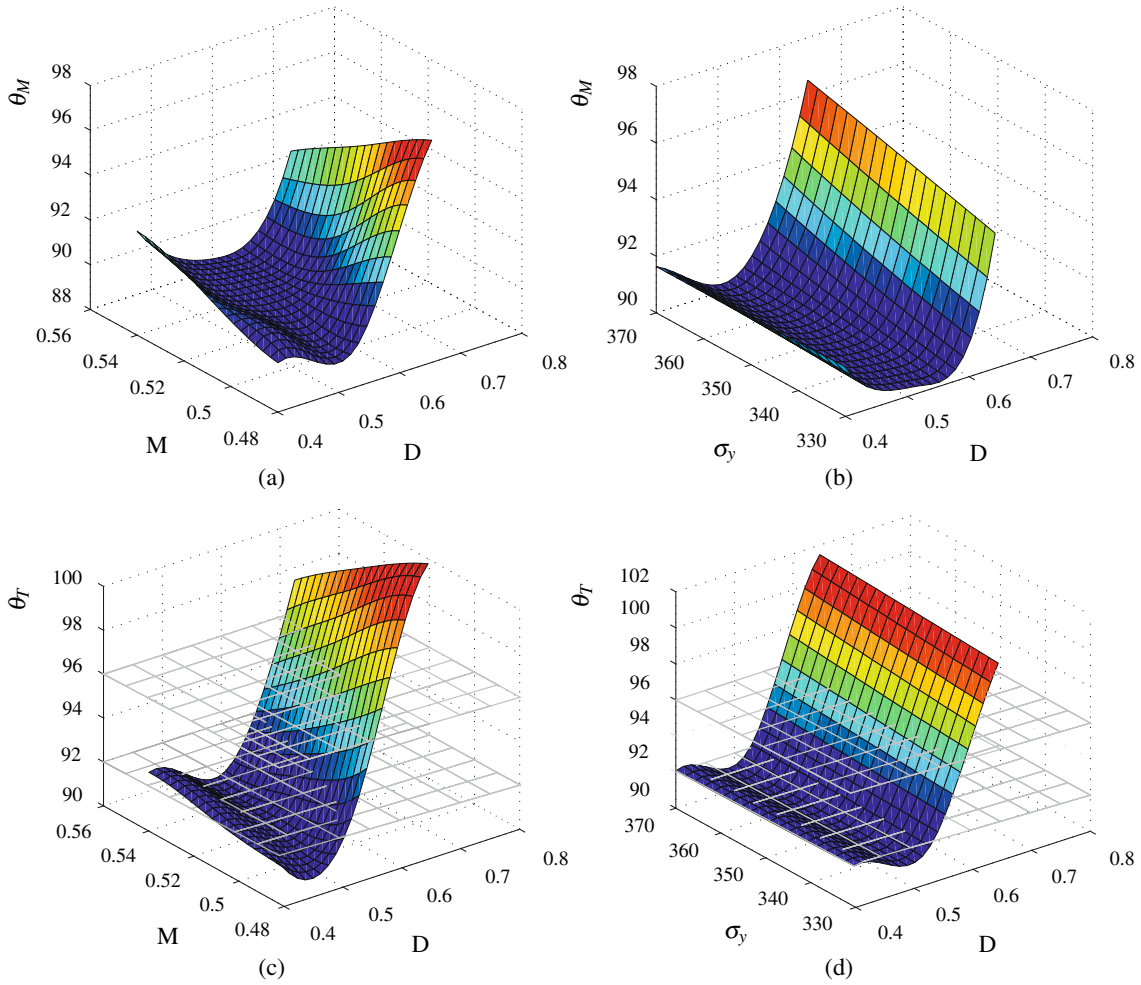

Fig. 11 Reference model impressions of the (**a**, **b**) main and (**c**, **d**) transition angle

Impressions of the reference models are shown in Fig. 11. Figure 11a and b show the reference model of the main angle as a function of the distance D, and the material thickness M and yield stress σ_y respectively. Figure 11c and d show the reference model of the transition angle as a function of the distance D, and the material thickness M and yield stress σ_y respectively. The constraints on the transition angle are visualized by the two planes. For visualization purposes, the remaining variables are set to their nominal process settings as shown in the second column of Table 3.

Evaluating the shape of the models in Fig. 11, an increase of the main angle is observed for large D. As long as the distance D is larger than the material thickness M, the material is only bent and not yet flattened. For increasing D, the material is less bended which results in an increase of the main angle. Once the distance D is smaller than the material thickness, the material is flattened subsequent to bending. Due to flattening of the material, the main angle will approach the nominal tooling angle of 92°. Also note the interaction effect between D and M in Fig. 11a and c. The slope in the noise variable direction changes as a function of D. In between the extreme settings of D, an area can be observed for which the slope in the noise variable direction is small. For this specific setting, this could potentially yield a process which is robust with respect to the noise variable M. Looking at Fig. 11b and d, again an area can be observed for which the noise variable σ_y has minimal influence on the main and transition angle respectively. Looking at the main effects of the plotted parameters, it can be observed that the depth setting has the highest effect on both angles followed by the material thickness and yield stress. This corresponds to the results of the sensitivity study described in Section 5.1.

Comparing the shape of the reference model with respect to the main angle (Fig. 11a and b) and the transition angle (Fig. 11c and d), a very similar behavior of the angle change can be observed. Note that especially the lower constraint on the transition angle, represented by the lower plane, significantly decreases the feasible area also excluding the robust area.

5.3 Robust optimization

The set of metamodels resulting from the different initial DOE sizes are subsequently used for robust optimization, solving (9). An initial optimization approach did not result in a $\pm 3\sigma$ process. This is caused by a non-robust behavior of the transition angle in the feasible design space and violation of the main angle USL. Therefore, both the objective and the $\pm 3\sigma$ constraints on the transition angle are slightly relaxed. The revised and reduced robust optimization formulation now reads:

$$
\begin{aligned}
&\text{find } \mathbf{x} \\
&\min\ |(\mu_{\theta_M} - 90)| + 2\sigma_{\theta_M} \\
&\text{s.t. } 92 \le \mu_{\theta_T} - 2\sigma_{\theta_T} \\
&\qquad \mu_{\theta_T} + 2\sigma_{\theta_T} \le 96 \\
&\qquad 92 \le \alpha \le 93 \\
&\qquad 0.4 \le D \le 0.65 \\
&\qquad 4 \le L_1 \le 5 \\
&\qquad 1 \le R_1 \le 1.3 \\
&\qquad M \sim \mathcal{N}(0.51, 0.01^2) \\
&\qquad \sigma_y \sim \mathcal{N}(350, 6.66^2)
\end{aligned}
\tag{10}
$$

The optimal value of the objective function obtained from each metamodel is represented by the first marker of each line in Fig. 12. For the 60LHD model, the optimal response values are given in the third column of Table 3. Moreover, the corresponding optimal process settings are included where f is the objective and g_1 and g_2 are the constraints on the transition angle. The reference model is subsequently utilized for robust optimization using similar techniques as applied onto the metamodels. The resulting optimal reference process settings and response values are presented in Fig. 12 and in the last column of Table 3. Evaluation of the nominal process settings (with $D = 0.51$ mm) using the reference model shows a very robust but unreliable process, see the second column of Table 3. A small standard

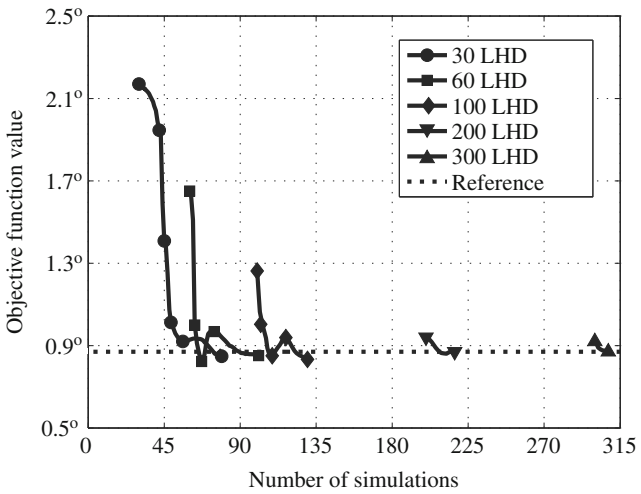

Fig. 12 Sequential robust optimization results for varying initial DOE sizes

Table 3 Current, optimized and reference process settings and response values of the V-bending process

Variables and responses	Nominal process settings	RO results	SRO results	Reference process settings
α	92°	92.4°	92.7°	92.8°
R_1	1.15 mm	1.16 mm	1.14 mm	1.12 mm
L_1	5 mm	4.8 mm	4.9 mm	4.9 mm
D	Varied	0.54 mm	0.55 mm	0.56 mm
f	0.63°	1.60°	0.85°	0.87°
g_1	90.2°	92.0°	92.0°	92.0°
g_2	91.1°	93.6°	94.9°	95.6°

The Robust Optimization (RO) results and Sequential Robust Optimization (SRO) results are obtained using the metamodel initially build up out of 60 DOE points

deviation for the transition angle response is observed but the lower constraint is violated by far.

Figure 13 presents the optimal process results for the main and transition angle as a function of D. The vertical bars represent the $\pm 2\sigma$ bounds of angle variation around the mean value caused by the influence of the noise variables. Based on the initial 60LHD model of the main angle presented in Fig. 13a, the optimal distance D is found to be 0.54 mm corresponding to a mean value of the main angle of 90.9° and a standard deviation of 0.35°. The resulting objective function value deviates 0.73° from the optimal reference value of 0.87°. This discrepancy is relatively large compared to the accuracy which is required from the V-bending process. Looking at the initial optimal values of the objective function values for the 30LHD and 100LHD metamodels as presented in Fig. 12, a deviation of 1.31° and 0.39° from the reference solution is observed respectively. The discrepancy clearly decreases with an increasing number of initial DOE points. Evaluation of the 200LHD and 300LHD model shows an accurate prediction of the initial optimal objective function value.

Once an optimum is obtained by the robust optimization strategy, the 2σ-requirements for the moment matching constraints on the transition angle are satisfied per definition. However, the constraint predictions are based on a metamodel approximation. The reference model can be used to validate the prediction of the optimal constraint values based on the 60LHD model. Figure 13b depicts an additional set of $\pm 2\sigma$ bars at $D = 0.54$ representing the 60LHD and reference model prediction. A comparison shows that the 60LHD model under predicts the standard deviation. For the 60LHD model, an initial robust optimum is found that satisfies the constraints whereas the reference model shows violation of the lower constraint. In the case of deterministic optimization, neglecting the influence of the noise variables will result in an optimum that lies at the boundary of the lower constraint on θ_T for $D = 0.53$ mm for the reference model. The variation in M and σ_y will in this case lead to a high number of violations of the constraint in the real V-bending process. From this, it can be concluded that the effect of adding noise is significant if one compares the deterministic to the robust optimal reference settings for D.

The above analysis shows that the optimal distance D, which is actively adapted in the current process, is critical with respect to the lower constraint. A comparison of the optimal setting based on the 60LHD model shows a shift from the nominal process setting towards the more robust reference setting (see Table 3). However, a small discrepancy remains present mainly caused by an inaccurate prediction of the stochastic constraint measures. Overall, it can be stated that the prediction of the optimal process behavior based on the 60LHD model deviates from the reference model for both the main and transition angle. This leaves room for the sequential robust optimization step to increase the accuracy of the standard deviation and mean value prediction in the robust optimum for both the objective function and constraints. Before applying the sequential robust optimization algorithm in Section 5.5, experimental validation of the numerical results is performed and described next.

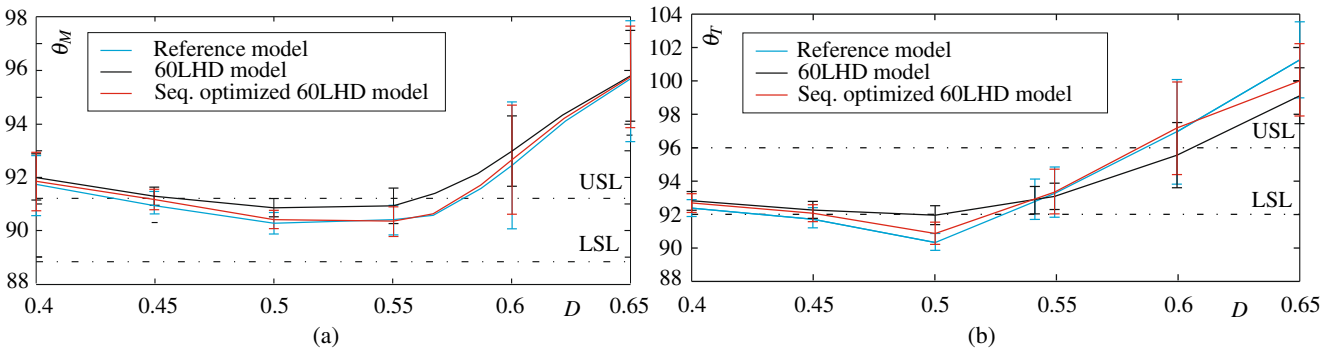

Fig. 13 Optimal process results for the **a** main and **b** transition angle as a function of the distance D

5.4 Experimental validation

To investigate the robustness of the nominal production process and to validate the numerical results, three production trial runs are performed with the nominal process settings as specified in Table 3 with $D = 0.53$ mm. To reflect the whole range of material thickness variation that can occur in practice, 3 material coils are selected with a minimum (Run 1), nominal (Run 2) and maximum (Run 3) material thickness within the $\mu \pm 3\sigma$ range as specified by the noise variable M in (10). This enables studying both the effect of coil-to-coil and in-coil thickness variation on the main and transition angle. For each trial run, 30 products are retrieved from the production process and the main and transition angles are measured.

The experimental results for the main and transition angle per trial run (Run 1–3) are visualized using box plots in Fig. 14a. The median of each set of 30 measurements is shown as the center line in the box. The boxes to the left and right of the median represent two quartiles containing 25% of the data points each. The horizontal line, or whisker, extends up to the lowest and highest measured value and covers the remaining 50% of the angle measurements. Possible outliers are measurements that fall outside the limits of the whiskers and are depicted as asterisks. In addition to the experimental results, a comparison is made with the numerical robustness prediction obtained by performing a MCA onto the reference model (Ref.) at the nominal process settings with $D = 0.53$ mm. See the lower box in Fig. 14a.

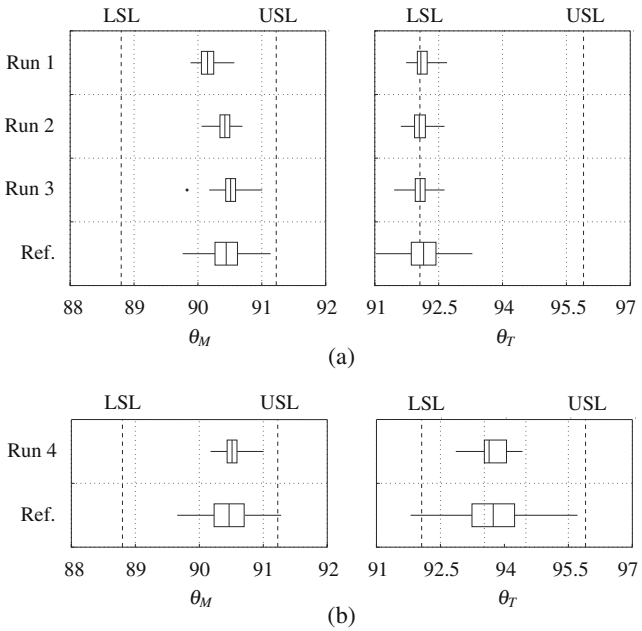

Fig. 14 Experimental results (Run 1–4) and numerical results obtained from the reference model (Ref.) for the nominal process settings with **a** $D = 0.53$ mm and **b** $D = 0.55$ mm

Evaluating the box plots in Fig. 14a, a larger effect of coil-to-coil variation is observed for the main angle in comparison to the transition angle. Looking at the main angle, springback increases for decreasing material thickness. Note that the springback angle is the difference between the measured angle and the nominal tooling angle of 92°. This effect corresponds to experimental V-die bending results reported in Osman et al. (2010). Both the mean value as well as the range of main angle variation is predicted accurately by the reference model. Also for the transition angle, the prediction of the mean value is in good agreement with the experimental results. However, the reference model shows a slight over prediction of the scatter around the mean value. As already predicted numerically and discussed in Section 5.3, also the experimental results show that the process performance is critical with respect to the lower specification limit of the transition angle.

Both the sensitivity study and the robust optimization procedure has shown that the main and transition angle are most significantly influenced by the depth setting D. To validate the numerical trends, a final trial run (Run 4) is performed whereby D is increased to 0.55 mm and the coil with a nominal material thickness is used. The experimental and numerical (Ref.) results are presented in Fig. 14b. For both angles, the numerical prediction of the mean value is in good agreement with the experimental results whereas the scatter around the mean value is over estimated. This discrepancy is expected to decrease if the number of measured products is increased and/or different coils are used in the production process. Note that the numerically observed trend of an increasing mean response of the transition angle for an increasing depth setting is confirmed by the experiments. This makes the process uncritical with respect to the lower specification limit of the transition angle.

In summary, the numerical trends obtained from the reference model are in good agreement with the experimental results, especially for the mean value prediction. Returning back to the initially created metamodel set, the numerical prediction of the optimal process behavior based on the 60LHD model deviates from the reference model and thus from the experimental results. The next step is to decrease this discrepancy by application of the sequential robust optimization algorithm.

5.5 Sequential robust optimization

The results of applying the sequential robust optimization procedure to the set of metamodels are presented in Fig. 12. A clear difference in behavior of the algorithm can be observed for the different metamodels. For the 30LHD metamodel, a slower initial convergence is obtained in comparison to the 60LHD and 100LHD model. Evaluation of the infill point locations for the 30LHD model shows that

the first 12 points are added globally. The limited initial DOE size forces the algorithm to first decrease the metamodels prediction error globally before searching locally. Decreasing the initial DOE size below 30 results in a low quality metamodel, unsuitable for evaluation of the EI criterion. In total 49 points are added to the initial 30 DOE points after which the EI drops below the threshold value, arbitrarily set to $\Delta_s = 0.5$. However, Fig. 12 shows that an accurate prediction of the objective function value is already obtained after adding 20 DOE points.

For the 60LHD metamodel, the EI algorithm mainly adds infill points clustering around the robust optimum. A fast convergence of the objective function value prediction is observed towards the reference solution. Note however that the 30LHD model outperforms the 60LHD model after having added 30 infill points. The same can be observed for the 60LHD model and the 100LHD model after adding 40 infill points to the 60 initial DOE points. In total, an additional 42, 30, 17 and 8 infill points are added to the 60LHD, 100LHD, 200LHD and 300LHD model respectively. The latter two models only show a minor improvement of the prediction accuracy.

The optimal process settings of the robust optimum based on the 60LHD model after sequential robust optimization, are given in the fourth column of Table 3. The optimal settings of α, R_1, D and especially L_1 have converged further towards the reference solution. The optimal process results obtained after sequential optimization of the 60LHD model are presented in Fig. 13a and b. The discrepancy between the sequentially updated metamodel prediction and the reference model is decreased significantly. Especially, the optimal values of the objective function and constraint based on the sequentially updated 60LHD model show good resemblance with the optimal reference values.

Overall, it can be stated that application of the sequential robust optimization strategy to the V-bending process resulted in a significant improvement of the robustness and reliability. The deteriorating effects of the noise variables are minimized by changing the tooling angle and increasing the process depth setting. This will make active control of the depth setting in the current process redundant. Moreover, many of the process insights have been obtained by visualization of the metamodels used in the robust optimization strategy. Finally, it is demonstrated that the sequential optimization step improves the accuracy of the response predictions at regions of interest in a very efficient way.

6 Conclusions and future work

In this paper, a robust optimization strategy is presented that allows for modeling and solving robust optimization problems using time-consuming numerical simulations. Uncertainties such as material variation and fluctuating process settings are taken into account explicitly. The resulting response variation of both the objective function and constraints is determined and accounted for in the strategy to optimize towards robust and reliable processes. The challenge remains to balance the number of time-consuming FE simulations spent on the robustness evaluation and the accuracy of the robustness predictions themselves. A sequential robust optimization step is applied based on an expected improvement measure to increase the efficiency of the strategy.

The robust optimization strategy is successfully applied to an analytical test function and industrial V-bending process. The potential of the strategy is demonstrated by modeling and sequentially solving these robust optimization problems. For the V-bending application, a significant improvement of the robustness ($> 2\sigma$) and reliability was obtained by accounting for the deteriorating effects of several noise variables. Moreover, experimental validation of the numerical robustness results shows a good agreement with the experimental results obtained by multiple production trial runs. This result fosters the usage of numerical robustness analyses and optimization in an early stage of product and process design. Finally, it is demonstrated that the sequential optimization step improves the accuracy of the objective function prediction at regions of interest in an efficient way.

When using numerical techniques to describe a physical process, the designer has to deal with sources of uncertainty like numerical noise and approximation errors. A fruitful area of future research is to extend the robust optimization strategy to account for these sources of uncertainty. More in general, research efforts will be focused on efficiently including different sources of uncertainty and process robustness during numerical optimization.

Acknowledgments This research was carried out under the project number M22.1.08303 in the framework of the Research Program of the Materials innovation institute (www.m2i.nl). The industrial partners co-operating in this research are gratefully acknowledged for their useful contributions to this research.

References

Barthelemy JFM, Haftka RT (1993) Approximation concepts for optimum structural design - a review. Struct Multidisc Optim 5:129–144

Belur BK, Grandhi RV (2004) Geometric deviations in forging and cooling operations due to process uncertainties. J Mat Proc Tech 152:204–214

Beyer HG, Sendhoff B (2007) Robust optimization - a comprehensive survey. Comput Methods Appl Mech Eng 196:3190–3218

Bonte MHA (2007) Optimisation strategies for metal forming processes. Phd thesis, University of Twente, Enschede, The Netherlands

Bonte MHA, van den Boogaard AH, Huétink J (2008) An optimisation strategy for industrial metal forming processes. Struct Multidisc Optim 35:571–586

Breyfogle III F (2003) Implementing six sigma; smarter solutions using statistical methods. Wiley, New York

Du X, Chen W (2000) Methodology for managing the effect of uncertainty in simulation-based design. AIAA Journal 38:1471–1477

Du X, Chen W (2002) Efficient uncertainty analysis methods for multidisciplinary robust design. AIAA Journal 40(3):545–552

Haldar A, Mahadevan S (2000) Probability, reliability and statistical methods in engineering design. Wiley, New York

Hancock W, Zayko M, Autio M, Ponagajba D (1997) Analysis of components of variation in automotive stamping processes. Qual Eng 10(1):115–124

Hopperstad O, Leira B, Remseth S, Tromberg E (1999) Reliability-based analysis of a stretch-bending process for aluminium extrusions. Comput Struct 71:63–75

Huang D (2005) Experimental planning and sequential kriging optimization using variable fidelity data. Phd thesis, Ohio State University, Columbus, Ohio, USA

Huang YM, Leu DK (1998) Effects of process variables on v-die bending process of steel sheet. Mech Sci 40:631–650

Jakumeit J, Herdy M, Nitsche M (2005) Parameter optimization of the sheet metal forming process using an iterative parallel Kriging algorithm. Struct Multidisc Optim 29:498–507

Jin R, Du X, Chen W (2003) The use of metamodeling techniques for optimization under uncertainty. Struct Multidisc Optim 25:99–116

Jones D, Schonlau M, Welch W (1998) Efficient global optimization of expensive black-box functions. J Glob Optim 13:455–492

Jurecka F, Ganser M, Bletzinger K (2007) Update scheme for sequential spatial correlation approximations in robust design optimisation. Comput Struct 85:606–614

Kang Z (2005) Robust design optimization of structures under uncertainties. Phd thesis, University of Stuttgart, Stuttgart, Germany

Kini SD (2004) An approach to integrating numerical and response surface models for robust design of production systems. Phd thesis, Ohio State University, Columbus, Ohio, USA

Kleiber M, Rojek J, Stocki R (2002) Reliability assessment for sheet metal forming operations. Comput Methods Appl Mech Eng 191:4511–4532

Kleiber M, Knabel J, Rojek J (2004) Response surface method for probabilistic assessment of metal forming failures. Numer Methods Eng 60:51–67

Koch PN, Yang RJ, Gu L (2004) Design for six sigma through robust optimization. Struct Multidisc Optim 26:235–248

Lehman JS (2002) Sequential design of computer experiments for robust parameter design. PhD thesis, Ohio State University, Columbus, Ohio, USA

Leu DK, Hsieh CM (2008) The influence of coining force on springback reduction in v-die bending process. J Mat Proc Tech 196:230–235

Li B, Nye T, Metzger DR (2005) Multi-objective optimization of forming parameters for tube hydroforming process based on the Taguchi method. Adv Manuf Technol 28:23–30

Möller B, Beer M (2008) Engineering computation under uncertainty - capabilities of non-traditional models. Comput Struct 86:1024–1041

Montgomery D (2005) Introduction to statistical quality control. Wiley, New York

Montgomery DC (2009) Design and analysis of experiments. Wiley, New York

Myers RH, Montgomery DC (2002) Response surface methodology. Wiley, New York

Osman MA, Shazly M, El-Mokaddem A, Wifi AS (2010) Springback prediction in v-die bending: modelling and experimentation. Journal of Achievements in Materials and Manufacturing Engineering 38(2):179–186

Padmanabhan R, Oliveira MC, Alves JL, Menezes LF (2007) Influence of process parameters on the deep drawing of stainless steel. Finite Elem Anal Des 43:1062–1067

Park GJ, Lee TH, Lee KH, Hwang KH (2006) Robust design: an overview. American Institute of Aeronautics and Astronautics 44:181–191

Repalle J, Grandhi RV (2005) Design of forging process variables under uncertainties. Materials Engineering and Performance 14:123–131

Sacks J, Welch WJ, Mitchell T, Wynn H (1989) Design and analysis of computer experiments. Stat Sci 4:409–423

Santner T, Williams B, Notz W (2003) The design and analysis of computer experiments. Springer Series in Statistics. Springer, ISBN 978-0-387-95420-2

Schonlau M (1997) Computer experiments and global optimization. Phd thesis, University of Waterloo, Ontario, Canada

Schuëller GI, Jensen HA (2008) Computational methods in optimization considering uncertainties - an overview. Comput Methods Appl Mech Eng 198:2–13

Taguchi G (1987) Systems of experimental design. Unipub/Kraus International Publication, White Plains, New York

Tekaslan O, Şeker U, Özdemir A (2006) Determining springback amount of steel sheet metal has 0.5 mm thickness in bending dies. Mater Des 27:251–258

Tekaslan O, Gerger N, Şeker U (2008) Determination of spring-back of stainless steel sheet metal in "V" bending dies. Mater Des 29:1043–1050

Williams B, Santner T, Notz W (2000) Sequential design of computer experiments to minimize integrated response functions. Stat Sin 10:1133–1152

Yang K, El-Haik B (2003) Design for six sigma; a roadmap for product development. McGraw-Hill, New York

Yildiz AR (2009) A new design optimization framework based on immune algorithm and Taguchi method. Comput Ind 60(8):613–620

Yildiz AR, Öztürk N, Kaya N, Öztürk F (2007) Hybrid multi-objective shape design optimization using Taguchi's method and genetic algorithm. Struct Multidisc Optim 34(4):317–332